

Misorientation angle dependence of the critical current in HTS bicrystals with low-angle [001]-tilt grain boundaries

A.L. Kasatkin and V.P. Tsvetkovskii

*G.V. Kurdyumov Institute of Metal Physics, National Academy of Sciences of Ukraine
36 Vernadsky Str., Kiev 03142, Ukraine
E-mail: al_kas@i.ua*

Received November 25, 2019, published online February 28, 2020

Dependence of the critical current on the misorientation angle in high-temperature superconductor (HTS) [001]-tilt bicrystal is theoretically examined. It's argued that in the case of relatively small values of the bicrystal misorientation angle θ ($\theta \leq 10\text{--}15^\circ$) the critical current as well as the resistive state emergence are determined by depinning of Abrikosov vortices, which are locked by c -oriented edge dislocations which form the low-angle [001]-tilt grain boundary and are aligned in a linear row along it. Dependence of the depinning critical current on the misorientation angle of bicrystal is calculated for this case and it reveals a good agreement with experimental data obtained on HTS bicrystals with low-angle [001]-tilt grain boundaries.

Keywords: superconductor, bicrystal, grain boundary, Abrikosov vortex, dislocation, pinning, critical current.

1. Introduction

High-temperature superconducting (HTS) materials produced on the base of “cuprate” compounds (RE)–Ba–Cu–O (RE is the rare-earth element: Y, Gd, Nd) are of great practical interest for electrical engineering and electronics [1]. First of all it concerns the possibility of large-scale applications, such as: superconducting electric power cables, high-field magnets, motors, energy storage devices, etc. This interest is caused by a large current carrying ability of HTS materials, allowing dissipation-free current flow with densities more than 10^6 A/cm² at liquid nitrogen temperature (77 K) and magnetic fields up to 10 T, obtained for HTS (RE)Ba₂Cu₃O_{7- δ} ((RE)BCO) films and coatings. Now significant efforts are aimed to improve production technology and current carrying characteristics of practically valuable HTS conductors — preferably in form of HTS tapes, deposited (over the special buffer layers) on flexible metallic substrates — so-called “second generation of HTS conductors” [2,3]. The most important task (both for physics and applications of superconductivity), which arises in these researches, is enlargement of the critical current density j_c and elimination of its dependence on magnetic field value and orientation, as well as on the HTS tape thickness [4–14].

Numerous studies performed on different HTS films and coatings with regard to their possible large-scale applications have unambiguously demonstrated that one of the most im-

portant structural features of these superconductors, which provides limitations on their current-carrying capability, is existence of grain boundaries (GB) within the material, playing the role of barriers for supercurrent flow [1,4,15–19]. This evidence principally comes from numerous transport studies performed on single grain boundaries in HTS bicrystals, usually obtained by deposition of HTS films on bicrystalline substrates. For HTS epitaxial thin films and highly textured coatings, which possess the highest j_c values and are mostly interesting for applications, the main type of GB, affecting the critical current value, are [001]-tilt grain boundaries, which correspond to rotation of neighboring crystalline grains on the both sides of GB around the c axis, which is perpendicular to the superconducting Cu–O planes (ab planes) of anisotropic (layered) HTS material and film/coating substrate.

This type of grain boundary in [001]-tilt bicrystal is schematically shown in Fig. 1. Experiments performed on [001]-tilt YBCO bicrystals [16–21] have demonstrated that the critical current density across the grain boundary depends strongly on the misorientation angle θ of grains, and drops nearly exponentially when θ increases: $j_c(\theta) \sim \exp(-\theta/\theta_c)$ where $\theta_c \approx 1\text{--}3^\circ$. It's well known, that low-angle [001]-tilt GB in YBCO bicrystals and c -oriented epitaxial films (coatings) may be considered as rows parallel to the c -axis edge dislocations [17,22–24]. The average distance between neighboring dislocations in the row, according to Franck's

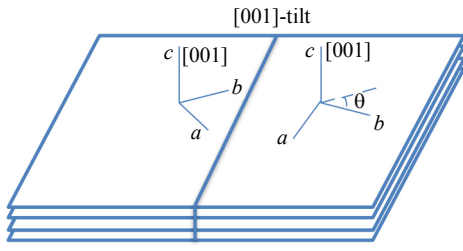


Fig. 1. Schematic sketch of the [001]-tilt bicrystal with a misorientation angle θ .

relation, strongly depends on the misorientation angle θ of neighboring grains in the ab plane: $d(\theta) \sim \theta^{-1}$, and by the order of magnitude usually lies in the range 3–10 nm.

At small θ values ($\theta \leq 10^\circ$), the dislocations which form the [001]-tilt GB are well separated. Therefore, in this case the current passes the GB through the nanosized channels between dislocation cores (Fig. 2), which are nonsuperconducting (dielectric or normal-metal cylindrical regions) owing to dislocation cores and strain fields around them [22]. On the other hand, at high θ values, a transition from strong to weak (Josephson) coupling of grains takes place. The Josephson properties of GB junctions in bicrystals with a high misorientation angle values have been widely studied (both experimentally and theoretically) [17,18].

In the present work we concentrate mostly on the behavior of GB junctions with a small misorientation angle values, providing the bulk current flow through the narrow channels between dislocation cores. One of the most interesting features of low-angle [001]-tilt GB in HTS films and bicrystals is the exponential type of $j_c(\theta)$ dependence for this kind of grain boundaries, as it was mentioned above. There are several theoretical models relating this type of $j_c(\theta)$ dependence with electron transparency of GB [25–27]. The latter, accordingly to these models, can drastically decrease with an increase of misorientation angle θ . Nevertheless, there is a strong experimental evidence that the cri-

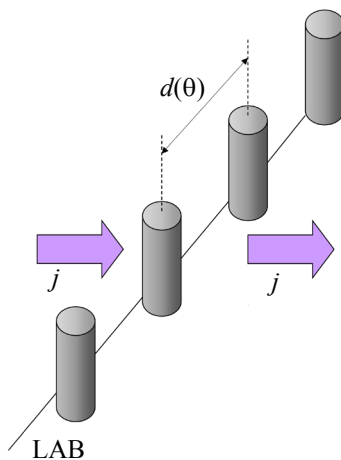


Fig. 2. Current flow through the [001]-tilt grain boundary in HTS.

tical current value through the GBs of this type, followed by simultaneous onset of the resistive state of superconductor, is tightly related with the start of vortex motion along the GB under the Lorentz force influence [28–34]. These vortices (Abrikosov, or mixed type — Abrikosov–Josephson (AJ) vortices [35]), which are locked within the [001]-tilt GB and pinned by dislocations, forming it. These vortices arise due to applied magnetic field, or can be self-induced by transport current flow. As a rule, the critical current for depinning of such kind vortices and onset of their motion under the Lorentz force action is essentially less than the depinning critical current for vortices, locked within grains. Thus, the GBs can form easy vortex flow channels in HTS films and bicrystals (as well as twin boundaries in HTS single crystals) [28,31–40].

In the present work the depinning critical current for periodic pinning potential created by a dislocation row along the [001]-tilt low-angle GB (LAB) in HTS bicrystal is calculated. The strong exponential $j_c(\theta)$ dependence for the critical current density is obtained for $\theta \geq 3^\circ$ at low magnetic field values (e.g., those induced by a transport current). The calculated $j_c(\theta)$ dependence matches quantitatively well with the corresponding experimental data, obtained for YBCO bicrystals [1,17,20,21], when the coherence length and the Burgers vector values determined from experiments [1,17] are used as a fitting parameters of the model. It is argued that for the case of [001]-tilt LAB the critical current density and, correspondingly, the onset of the resistivity are determined by depinning processes of magnetic flux quanta locked within the LAB and their subsequent flow along it at higher transport current values under the Lorentz force influence. In the framework of suggested model the main features of experimentally observed $j_c(\theta)$ dependence, such as plateau at low angles and exponential decrease at higher angle values, follow from the specific form of periodic vortex pinning potential, created by the equidistant edge dislocations row, which forms the [001]-tilt LAB in HTS bicrystal [1,17,22–25].

2. Model and results

In this section the depinning critical current value is calculated for the case of periodic pinning potential $U_p(\mathbf{s})$, created by a linear row of parallel equidistant c -oriented edge dislocations, forming the low-angle [001]-tilt grain boundary (LAB) along the x axis in HTS film or bicrystal. Following the works [41,42], the general expression for the pinning potential $U_p(\mathbf{s})$ in the framework of the Ginzburg–Landau theory can be written in form

$$U_p(\mathbf{s}) = -\int V_p(\mathbf{r}) \left[1 - \left| \frac{\psi(\mathbf{r}-\mathbf{s})}{\psi_\infty} \right|^2 \right] d^2\mathbf{r}. \quad (1)$$

Here $\psi(\mathbf{r})$ is the order parameter of superconductor; $V_p(\mathbf{r})$ is the depairing potential for electrons, which characterizes

the materials inhomogeneity, leading to the local suppression of superconductivity. Within the model of δT_c -pinning an expression for $V_p(\mathbf{r})$ can be written in form [41]: $V_p(\mathbf{r}) = |\psi_\infty|^2 \delta\alpha(\mathbf{r})$, where $\alpha \equiv \alpha'(T - T_c)$ is the parameter of the Ginzburg–Landau theory. In the case of periodic potential $V_p(\mathbf{r})$, produced by dislocation row along the grain boundary, we will use an approximation

$$V_p(\mathbf{r}) = \sum_n V_{p0}(\mathbf{r} - n\mathbf{d}), \quad V_{p0}(\mathbf{r}) = V_0 \pi r_p^2 \delta_2(\mathbf{r}).$$

For the row of c -oriented edge dislocations with a Burgers vector \mathbf{b} , which forms the low-angle [001]-tilt grain boundary (LAB) in HTS film or bicrystal, the distance between neighboring dislocations is determined by the Franck's relation:

$$d = \frac{b}{2 \sin(\theta/2)}, \quad \mathbf{d} = d\hat{\mathbf{x}}, \quad b = |\mathbf{b}|. \quad (2)$$

Besides that, in Eq. (1) we will use a well known relation for the local change of the order parameter $\psi(r)$ in vicinity of the Abrikosov vortex core on the scale of the coherence length ξ [41]:

$$f(r) = \frac{|\psi(r)|}{|\psi_\infty|} \equiv \frac{r}{\sqrt{r^2 + 2\xi^2}}.$$

Using these assumptions, for the pinning potential $U_p(\mathbf{s})$, given by Eq. (1), one can obtain

$$\begin{aligned} U_p(\mathbf{s}) &= -V_0 \pi r_p^2 \int d^2r \sum_n \delta_2(\mathbf{r} - n\mathbf{d}) \left[1 - \frac{(\mathbf{r} - \mathbf{s})^2}{(\mathbf{r} - \mathbf{s})^2 + 2\xi^2} \right] = \\ &= -V_0 \pi r_p^2 \sum_n \frac{2\xi^2}{(nd + s_x)^2 + s_y^2 + 2\xi^2}, \quad (3) \\ d &\equiv d(\theta) = \frac{b}{2 \sin(\theta/2)}. \end{aligned}$$

Performance of summation in Eq. (3) using the well-known expression for the sum of series:

$$\sum_{k=-\infty}^{\infty} 1/(k+a) = \pi \operatorname{ctg}(\pi a)$$

gives the following result for the periodic pinning potential $U_p(\mathbf{s})$ determined by (3) [42] and shown in Fig. 3:

$$\begin{aligned} U_p(\mathbf{s}) &= -V_0 \pi r_p^2 \frac{2\pi\xi^2}{d\sqrt{s_y^2 + 2\xi^2}} \times \\ &\times \frac{\operatorname{sh}\left(2\pi\sqrt{s_y^2 + 2\xi^2}/d\right)}{\operatorname{ch}\left(2\pi\sqrt{s_y^2 + 2\xi^2}/d\right) - \cos(2\pi s_x/d)}. \quad (4) \end{aligned}$$

From Eq. (4) it follows, that the periodic pinning potential in the plane of grain boundary $U_p(s_x)$ has the form

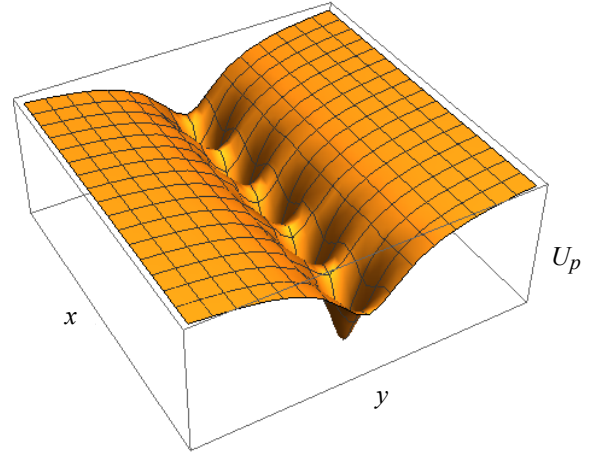


Fig. 3. (Color online) Pinning potential $U_p(\mathbf{s})$ calculated from Eq. (4).

$$U_p(s_x) = -V_0 \pi r_p^2 \frac{\sqrt{2}\pi\xi}{d} \frac{\operatorname{sh}\left(2\sqrt{2}\pi\xi/d\right)}{\operatorname{ch}\left(2\sqrt{2}\pi\xi/d\right) - \cos(2\pi s_x/d)}. \quad (5)$$

The pinning potential determined by Eqs. (4), (5) depends on the misorientation angle θ of neighboring crystalline blocks, separated by a grain boundary. This dependence is determined by the $d(\theta)$ relation given by Eq. (2). This in turn allows to calculate the angular dependence of the critical current density, $j_c(\theta)$, determined by depinning of vortices, locked within the grain boundary

$$j_c(\theta) = \frac{1}{\phi_0} \max \left(\frac{\partial U_p}{\partial s_x} \right). \quad (6)$$

It worse to notice that in thick superconducting films or plates with a thickness $D > \lambda$ (λ is the London penetration depth) Eq. (6) determines the critical current density on the specimen surface: when the surface current density reaches the critical value, the instability of vortex pinning state emerges and process of vortex escape from linear defect (dislocation) under the Lorentz force influence starts at the surface and subsequently propagates inside the specimen [43,44] (see Fig. 4). At high enough temperatures $T \leq T_c$ transfer of elastic vortex strings along the edge dislocations row, forming the low-angle [001]-tilt grain boundary can proceed due to thermally activated vortex kinks motion which provide transfer of vortex strings between neighboring dislocations in the row along the grain boundary. In the TAFF regime of vortex strings one can also expect the exponential dependence of $j_c(\theta)$ compatible with experimental data [45].

Numerical calculation of $j_c(\theta)$ dependence from Eqs. (5), (6) leads to the result presented in Fig. 5 in a semi-log scale. The following parameters values, corresponding to the case of YBCO bicrystals (see, e.g., [1,17,20]): $b = 0.4$ nm, $\xi = 2$ nm, were used for this calculation. The obtained result for $j_c(\theta)$ dependence agrees well with experimental data for YBCO bicrystals with [001]-tilt LAB as well as

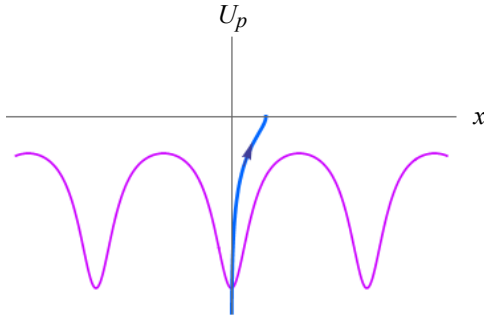


Fig. 4. Periodic pinning potential of dislocation [001]-tilt LAB in HTS bicrystal. The bended solid line with an arrow on its end represents an elastic vortex string exerted to the Lorentz force action inhomogeneously distributed near the specimen surface within the layer of width λ .

for similar type bicrystals produced from other kind superconducting materials, e.g., ferropnictides [46,47]. In accordance to experimental data obtained on YBCO [001]-tilt bicrystals, the most specific features of this dependence are: (a) existence of plateau at small misorientation angles ($\theta < 2-4^\circ$) and (b) exponential decrease of $j_c(\theta)$ value with increase of θ at higher angles: $j_c(\theta) \sim \exp(-\theta/\theta_0)$ (typically $\theta_0 = 3-5^\circ$) [1,17,19–21]. As one can see from Fig. 4, the calculated $j_c(\theta)$ dependence reveals both these features, thus it describes qualitatively well the experimental results. Similar results (but with slightly higher values of the initial plateau and θ_0 value for exponential $j_c(\theta)$ dependence) were observed for ferropnictides [001]-tilt bicrystals [46,47].

3. Conclusion

In the present work it is argued that limitation of current carrying capability in HTS epitaxial thin films and bicrystals with low-angle [001]-tilt grain boundaries (LAB) at not too large misorientation angle values ($\theta \leq 10-15^\circ$) is determined by depinning of Abrikosov (or Abrikosov–Josephson) vortices, which are locked by linear rows of edge dislocations, forming such kind of grain boundaries. In this case

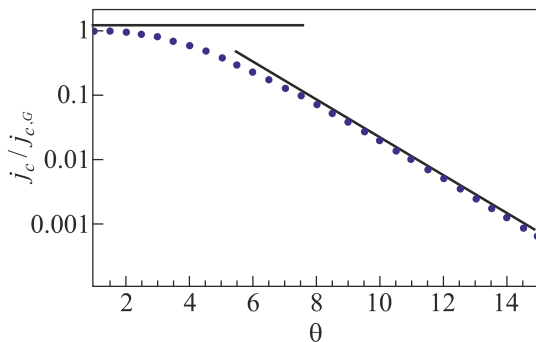


Fig. 5. Calculated dependence of the depinning critical current density $j_c(\theta)$ on the misorientation angle θ for dislocation [001]-tilt LAB in HTS bicrystal (normalized on the intragrain critical current density value).

the resistive state arises due to vortex transfer along the dislocation row in the grain boundary, perpendicularly to the transport current flow through it. We consider the problem of vortex depinning and corresponding depinning critical current in a single-vortex approximation, thus neglecting the intervortex interaction. For the case of rather thick films ($D > \lambda$) this approximation corresponds to the case of intervortex distances $a_\phi(H) > \lambda$. The latter takes place at $H < H_{c1}$. We suppose that this inequality is fulfilled. Usually in experiments on HTS bicrystals, particularly in those, which we refer in the present work, the $j_c(\theta)$ dependence is measured in the self-field of a transport current flowing through the grain boundary, which is much smaller than H_{c1} . In the case of applied dc magnetic field the intervortex interaction can significantly affect the critical current value flowing through the grain boundary. It is known from theoretical and experimental investigations both for low-angle boundaries with a bulk current flow, like that in [001]-tilt bicrystals [48–51], and also for Josephson junctions, where Josephson vortices in the junction interact with Abrikosov vortices in the banks and this significantly changes the Fraunhofer-type Josephson critical current dependence on applied magnetic field $J_{c,f}(H)$ [52–54].

In the framework of considered model with a suitable ξ and b parameters values we have demonstrated, that dependence of the critical current density on the misorientation angle $j_c(\theta)$ in low-angle [001]-tilt HTS bicrystals is characterized by existence of a plateau at small angles ($\theta \leq 2-4^\circ$) followed by an exponential dependence of the type: $j_c(\theta) \sim \exp(-\theta/\theta_0)$ with characteristic values $\theta_0 = 1-3^\circ$ ($\theta_0 \approx 1.7^\circ$, as it is demonstrated in Fig. 5 of the present paper). The only parameters which determine this dependence in the framework of considered model are the coherence length ξ , and the Burgers vector modulus b . Their values for numerical calculation accordingly to Eqs. (3)–(6) we took from experimental works (see the text). In experiments performed on HTS bicrystals with low-angle [001]-tilt grain boundaries quite similar dependences for $j_c(\theta)$ were obtained with a plateau at small angles θ and exponential decay at higher misorientation angles. For YBCO and BiSCCO [001]-tilt bicrystals the θ_0 value which characterizes the exponential decay law for $j_c(\theta)$ dependence is somewhat higher than that we have obtained numerically: $\theta_0 = 3-5^\circ$ in experiments [1,17,20] and this value is even higher for ferropnictides bicrystals with [001]-tilt grain boundaries. Thus, the model for depinning critical current in the case of periodic pinning potential supplied by a linear dislocation row allows to achieve a qualitative agreement between the calculated $j_c(\theta)$ dependence and corresponding experimental dependence, obtained for HTS ($\text{YBa}_2\text{Cu}_3\text{O}_{7-\delta}$) and ferropnictides bicrystals with [001]-tilt grain boundaries, while quantitative discrepancy, as we suppose, may be related with an incorrect choice of parameters ξ and b .

The model presented here may be extended to account for other types of periodic pinning potential in superconduc-

tors: modulated 1D channels for vortex guiding [55,56], set of parallel grooves for the case of vortex motion across them [57,58], regular arrays of antidots or magnetic dots [59–64]. For each of these cases the problem will consist in a correct choice of the pinning potential $U_p(\mathbf{s})$, instead of that given by Eqs. (3)–(5) and used in the present work.

The studies were supported by the National Academy of Sciences of Ukraine within the budget program KPKBK 6541230–1A “Support for the development of priority areas of scientific research”.

1. D. Larbalestier, A. Gurevich, D.M. Feldmann, and A. Polyanskii, *Nature* **414**, 368 (2001).
2. S.R. Foltyn, L. Civale, J.L. MacManus-Driscoll, Q.X. Jia, B. Maiorov, H. Wang, and M. Maley, *Nature Mater.* **6**, 631 (2007).
3. B. Maiorov, S.A. Baily, H. Zhou, O. Ugurlu, J.A. Kennison, P.C. Dowden, T.G. Holesinger, S.R. Foltyn, and L. Civale, *Nature Mater.* **8**, 398 (2009).
4. K. Matsumoto and P. Mele, *Supercond. Sci. Technol.* **23**, 014001 (2010).
5. X. Obradors, T. Puig, A. Palau, A. Pomar, F. Sandiumenge, P. Mele, and K. Matsumoto, in: *Comprehensive Nanoscience and Technology*, Vol. 3, Elsevier, Amsterdam (2011), p. 303.
6. M. Miura, B. Maiorov, J.O. Willis, T. Kato, M. Sato, T. Izumi, Y. Shiohara, and L. Civale, *Supercond. Sci. Technol.* **26**, 035008 (2013).
7. X. Obradors and T. Puig, *Supercond. Sci. Technol.* **27**, 044003 (2014).
8. P. Mele, A. Crisan, and M.I. Adam, *Pinning-Engineered YBa₂Cu₃O_x Thin Films*, in: *Vortices and Nanostructured Superconductors*, A. Crisan (ed.), Springer Series in Materials Science, Vol. 261, Springer, Cham (2017), p. 15.
9. W.K. Kwok, U. Welp, A. Glatz, A.E. Koshelev, K.J. Kihlstrom, and G.W. Crabtree, *Rep. Prog. Phys.* **79**, 116501 (2016)
10. R. Wördenweber, *Phys. Sci. Rev.* **2**, No. 8 (2017).
11. I.A. Sadovskyy, Y. Jia, M. Leroux, J. Kwon, H. Hu, L. Fang, C. Chaparro, S. Zhu, U. Welp, J.-M. Zuo, Y. Zhang, R. Nakasaki, V. Selvamanickam, G.W. Crabtree, A.E. Koshelev, A. Glatz, and W.-K. Kwok, *Adv. Mater.* **28**, 4593 (2016).
12. I.A. Sadovskyy, A.E. Koshelev, W.-K. Kwok, U. Welp, and A. Glatz, *Proc. Natl. Acad. Sci. U.S.A. (PNAS)* **116**, 10291 (2019).
13. A.K. Jha and K. Matsumoto, *Front. Phys.* **7**, 82 (2019).
14. L. Civale, *Proc. Natl. Acad. Sci. U.S.A. (PNAS)* **116**, 10201 (2019).
15. J.E. Evetts, *Supercond. Sci. Technol.* **17**, S315 (2004).
16. J.H. Durrell and N.A. Rutter, *Supercond. Sci. Technol.* **22**, 013001 (2009).
17. H. Hilgenkamp and J. Mannhart, *Rev. Mod. Phys.* **74**, 485 (2002).
18. F. Tafuri and J.R. Kirtley, *Rep. Prog. Phys.* **68**, 2573 (2005).
19. D.M. Feldmann, T.G. Holesinger, R. Feenstra, C. Cantoni, W. Zhang, M. Rupich, X. Li, J.H. Durrell, A. Gurevich, and D.C. Larbalestier, *J. Appl. Phys.* **102**, 083912 (2007).
20. N.F. Heinig, R.D. Redwing, J.E. Nordman, and D. Larbalestier, *Phys. Rev. B* **60**, 1409 (1999).
21. R. Held, C.W. Schneider, J. Mannhart, L.F. Allard, K.L. More, and A. Goyal, *Phys. Rev. B* **79**, 014515 (2009).
22. S.E. Babcock and J.L. Vargas, *Annu. Rev. Mater. Sci.* **25**, 193 (1995).
23. C.-Y. Yang, S.E. Babcock, A. Ichinose, A. Goyal, D.M. Kroeger, D.F. Lee, F.A. List, D.P. Norton, J.E. Mathis, M. Paranthaman, and C. Park, *Physica C* **377**, 333 (2002).
24. I.-F. Tsu, J.-L. Wang, D.L. Kaiser, and S.E. Babcock, *Physica C* **306**, 163 (1998).
25. A. Gurevich and E.A. Pashitskii, *Phys. Rev. B* **57**, 13878 (1998).
26. G. Deutscher, *Appl. Phys. Lett.* **96**, 122502 (2010).
27. S. Graser, P.J. Hirschfeld, T. Kopp, R. Gutser, B.M. Andersen, and J. Mannhart, *Nature Phys.* **6**, 609 (2010).
28. B. Kalisky, J.R. Kirtley, E.A. Nowadnick, R.B. Dinner, E. Zeldov, Ariando, S. Wenderich, H. Hilgenkamp, D.M. Feldmann, and K.A. Moler, *Appl. Phys. Lett.* **94**, 202504 (2009).
29. A. Diaz, L. Mechin, P. Berghuis, and J.E. Evetts, *Phys. Rev. Lett.* **80**, 3855 (1998).
30. M.J. Hogg, F. Kahlmann, E.J. Tarte, Z.H. Barber, and J.E. Evetts, *Appl. Phys. Lett.* **78**, (2001).
31. A. Diaz, L. Mechin, P. Berghuis, and J.E. Evetts, *Phys. Rev. B* **58**, R2960 (1998).
32. J.H. Durrell, M.J. Hogg, F. Kahlmann, Z.H. Barber, M.G. Blamire, and J.E. Evetts, *Phys. Rev. Lett.* **90**, 247006 (2003).
33. T. Horide and K. Matsumoto, *Phys. Rev. B* **77**, 132502 (2008).
34. T. Horide, K. Matsumoto, Y. Yoshida, M. Mukaida, A. Ichinose, and S. Horii, *Physica C* **463–465**, 678 (2007).
35. A. Gurevich, *Phys. Rev. B* **65**, 214531 (2002).
36. V.M. Pan, G.G. Kaminsky, A.L. Kasatkin, M.A. Kuznetsov, V.G. Prokhorov, and C.G. Tretiatchenko, *IEEE Trans. Magn.* **27**, 1021 (1991).
37. V.V. Chabanenko, A.A. Prodan, V.A. Shklovskij, A.V. Bondarenko, M.A. Obolenskii, H. Szymczak, and S. Piechota, *Physica C* **314**, 133 (1999).
38. V.A. Shklovskij and O.V. Dobrovolskiy, *Phys. Rev. B* **74**, 104511 (2006).
39. O.K. Soroka, V.A. Shklovskij, and M. Huth, *Phys. Rev. B* **76**, 014504 (2007).
40. R. Besseling, T. Dröse, V.M. Vinokur, and P.H. Kes, *Europhys. Lett.* **62**, 419 (2003).
41. G. Blatter, M.V. Feigel'man, V.B. Geshkenbein, A.I. Larkin, and V.M. Vinokur, *Rev. Mod. Phys.* **66**, 1125 (1994).
42. E.A. Pashitskii and V.I. Vakaryuk, *Fiz. Nizk. Temp.* **28**, 16 (2002) [*Low Temp. Phys.* **28**, 11 (2002)].
43. V.A. Fedirko, A.L. Kasatkin, and S.V. Polyakov, *Phys. Metals Metallogr.* **117**, 864 (2016).
44. V.A. Fedirko, A.L. Kasatkin, and S.V. Polyakov, *J. Low Temp. Phys.* **192**, 359 (2018).
45. A.L. Kasatkin, V.M. Pan, and H.C. Freyhardt, *IEEE Trans. Appl. Supercond.* **7**, 1588 (1997).
46. T. Katase, Y. Ishimaru, A. Tsukamoto, H. Hiramatsu, T. Kamiya, K. Tanabe, and H. Hosono, *Nature Commun.* **2**, No. 409, 1 (2011).

47. J.H. Durrell, C.-B. Eom, A. Gurevich, E.E. Hellstrom, C. Tarantini, A. Yamamoto, and D.C. Larbalestier, *Rep. Prog. Phys.* **74**, 124511 (2011).
48. A. Gurevich and L.D. Cooley, *Phys. Rev. B* **50**, 13563 (1994).
49. X.Y. Cai, A. Gurevich, I.-Fei Tsu, D.L. Kaiser, S.E. Babcock, and D.C. Larbalestier, *Phys. Rev. B* **57**, 10951 (1998).
50. D. Kim, P. Berghius, M.B. Field, D.J. Miller, K.E. Gray, R. Feenstra, and D.K. Christen, *Phys. Rev. B* **62**, 12505 (2000).
51. A. Gurevich, M.S. Rzchowski, G. Daniels, S. Patnaik, B.M. Hinaus, F. Garillo, F. Tafuri, and D.C. Larbalestier, *Phys. Rev. Lett.* **88**, 097001 (2002).
52. M.V. Fistul', *Sov. Phys. JETP* **69**, 209 (1989).
53. V.N. Gubankov, M.P. Lisitskii, J.L. Serpuchenko, and M.V. Fistul', *Sov. Phys. JETP* **73**, 734 (1991).
54. M.V. Fistul' and G.F. Giuliani, *Phys. Rev. B* **58**, 9343 (1998).
55. K. Yu, M.B.S. Hesselberth, P.H. Kes, and B.L.T. Plourdel, *Phys. Rev. B* **81**, 184503 (2010).
56. R. Wördenweber, E. Hollmann, J. Schubert, R. Kutzner, and G. Panaitov, *Phys. Rev. B* **85**, 064503 (2012).
57. O.V. Dobrovolskiy and M. Huth, *Appl. Phys. Lett.* **106**, 142601 (2015).
58. O.V. Dobrovolskiy, V.M. Bevez, E. Begun, R. Sachser, R.V. Vovk, and M. Huth, *Phys. Rev. Appl.* **11**, 054064 (2019).
59. J.C. Keay, P.R. Larson, K.L. Hobbs, M.B. Johnson, J.R. Kirtley, O.M. Auslaender, and K.A. Moler, *Phys. Rev. B* **80**, 165421 (2009).
60. P. Sabatino, C. Cirillo, G. Carapella, M. Trezza, and C. Attanasio, *J. Appl. Phys.* **108**, 053906 (2010).
61. A.V. Silhanek, L. Van Look, R. Jonckheere, B.Y. Zhu, S. Raedts, and V.V. Moshchalkov, *Phys. Rev. B* **72**, 014507 (2005).
62. I. Swiecicki, C. Ulysse, T. Wolf, R. Bernard, N. Bergeal, J. Briatico, G. Faini, J. Lesueur, and J.E. Villegas, *Phys. Rev. B* **85**, 224502 (2012).
63. A. Hoffmann, P. Prieto, and I.K. Schuller, *Phys. Rev. B* **61**, 6958 (2000).
64. M.J. van Bael, L. van Look, K. Temst, M. Lange, J. Bekaert, U. May, G. Guntherodt, V.V. Moshchalkov, and Y. Bruynseraede, *Physica C* **332**, 12 (2000).

Залежність критичного струму від кута розорієнтації у бікрystalлах ВТНП із малокутовими межами нахилу [001]

О.Л. Касаткін, В.П. Цвітковський

Теоретично досліджено залежність критичного струму від кута розорієнтації бікрystalлу високотемпературного надпровідника (ВТНП) з межею нахилу [001]. Показано, що в разі відносно малих значень кута розорієнтації θ ($\theta \leq 10\text{--}15^\circ$) критичний струм, а також виникнення резистивного стану, визначаються депіннігом вихорів Абрикосова, захоплених s -орієнтованими крайовими дислокаціями, які утворюють малокутову межу нахилу [001] і вишикувані у лінійний ряд уздовж неї. Для цього випадку розрахована залежність критичного струму депіннігу від кута розорієнтації бікрystalлу, яка демонструє добре узгодження з експериментальними даними, отриманими на бікрystalлах ВТНП із малокутовими межами нахилу [001].

Ключові слова: надпровідник, бікрystalл, межа зерен, вихор Абрикосова, дислокація, пінніг, критичний струм.

Зависимость критического тока от угла разориєнтации в бикрystalлах ВТСП с малоугловыми границами наклона [001]

А.Л. Касаткин, В.П. Цветковский

Теоретически исследована зависимость критического тока от угла разориєнтации бикрystalла високотемпературного сверхпроводника (ВТСП) с границей наклона [001]. Показано, что в случае относительно малых значений угла разориєнтации θ ($\theta \leq 10\text{--}15^\circ$) критический ток, а также возникновение резистивного состояния определяются депиннингом вихрей Абрикосова, захваченных s -ориєнтованными краевыми дислокациями, которые образуют малоугловую границу наклона [001] и выстроены в линейный ряд вдоль нее. Для этого случая рассчитана зависимость критического тока депиннинга от угла разориєнтации бикрystalла, которая демонстрирует хорошее согласие с экспериментальными данными, полученными на бикрystalлах ВТСП с малоугловыми границами наклона [001].

Ключевые слова: сверхпроводник, бикрystalл, граница зерен, вихрь Абрикосова, дислокация, пиннинг, критический ток.